Classical Simulations Including Electron Correlations for Sequential Double Ionization

Yueming Zhou,[1] Cheng Huang,[1] Qing Liao,[1] and Peixiang Lu[1,2,*]

[1]*Wuhan National Laboratory for Optoelectronics and School of Physics, Huazhong University of Science and Technology, Wuhan 430074, People's Republic of China*

[2]*Key Laboratory of Fundamental Physical Quantities Measurement of Ministry of Education, Wuhan 430074, People's Republic of China*

(Received 29 February 2012; published 2 August 2012)

With a classical ensemble model that includes electron correlations during the whole ionization process, we investigate strong-field sequential double ionization of Ar by elliptically polarized pulses at the quantitative level. The experimentally observed intensity-dependent three-band or four-band structures in the ion momentum distributions are well reproduced with this classical model. More importantly, the experimentally measured ionization time of the second electrons by A. N. Pfeiffer *et al.* [Nature Phys. **7**, 428 (2011)], which cannot be predicted by the standard independent-electron model, is quantitatively reproduced by this fully classical correlated model. The success of our work encourages classical descriptions and interpretations of the complex multielectron effects in strong-field ionization where nonperturbative quantum approaches are currently not feasible.

DOI: 10.1103/PhysRevLett.109.053004 PACS numbers: 32.80.Rm, 31.90.+s, 32.80.Fb

Among various intense laser-induced phenomena, strong-field double ionization (DI) is one of the most important and fundamental processes. During the past decades, a great number of experimental as well as theoretical studies have been performed in this area. It has been known that DI proceeds either sequentially or nonsequentially. In nonsequential double ionization (NSDI), the second electron is ionized by the recollision of the first tunneled electron [1,2]. Because of this recollision, the two electrons from NSDI exhibit a highly correlated behavior [3–9]. In sequential double ionization (SDI), it is usually assumed that no correlation exists between the two electrons, and thus the ionization of the electrons can be treated as two independent tunneling-ionization steps. However, this assumption has been called into doubt by recent experiments [10,11]. In Ref. [10], it has been shown that there is a clear angular correlation between the two electrons from SDI, which implies that the successive ionization steps are not independent in SDI. In Ref. [11], the authors found that the ionization time of the second electron from SDI is much earlier than the prediction of the independent-electron model. These observations declare that the electron correlations in SDI should be reexamined carefully.

Theoretically, an accurate description of the electron correlations in DI needs full quantum theory. However, full-dimensional calculation of the time-dependent Schrödinger equation of the two- and multielectron systems requires enormous computational resources and it has only been performed on DI driven by the linear laser pulses [12]. Instead, numerous studies have resorted to classical methods [13–15]. For instance, a fully classical treatment of the two- and multielectron systems proposed by Eberly *et al.* has been well established [16–19]. During the past decade, this model has been successful in exploring the strong-field ionization processes at the qualitative level. However, it fails when made a quantitative comparison with experiments. For example, in Ref. [20] it has been shown that the saturation intensity for SDI of Ar in the classical simulation is much higher than the experimental data [11], and the amplitude of oscillation in the ratio of the parallel to antiparallel emitted SDI counts as a function of intensity is much larger than the experimental observation [21]. The following question remains: can a classical treatment describe the strong-field processes at the quantitative level [22]? In this Letter, we give an affirmative answer. With a delicate modification to Eberly's model, we performed a first quantitative simulation on strong-field SDI of Ar in the close-to-circular laser fields. Our numerical results exhibit intensity-dependent three-band or four-band structures in the ion momentum distributions, which are consistent with the recent experimental results [11]. Especially, the experimentally measured ionization time of the second electron [11], which cannot be predicted by the standard independent-electron model, is reproduced surprisingly well with this purely classical model which fully takes into account the electron correlations during the entire SDI process. The quantitative agreement between our numerical results and experimental data indicates that a classical treatment is a good approximation in describing the strong-field SDI and has the potential to shed light on the subtle multielectron effect in strong-field double and multiple ionizations.

In the classical picture of a two-electron system, one electron often drops deeply into the nuclear potential well, leading to the autoionization of the other electron. In Eberly's classical model [16,17], a soft-core potential is introduced for the ion-electron interaction to avoid autoionization. However, in this soft-core potential classical model (SPCM), the first and second ionization potentials cannot be matched with those of the investigated

target. In fact, the first electron often ionizes, leaving the second electron with an energy much lower than the second ionization potential of the target [23,24]. In tunneling and over-the-barrier ionization, the ionization rate is very sensitive to the ionization energy. Thus, the SPCM may be deficient in describing the strong-field double ionization that occurs through tunneling or over-the-barrier escape. However, this deficiency can be avoided with the Heisenberg-core potential, which not only prevents autoionization but also gives the ground-configuration energies of the multielectron atoms [25]. In the past decades, this potential has been extensively employed in the classical investigations of atomic and molecular collisions and laser-matter interactions [26,27]. Here, we employ the Heisenberg-core potential instead of the soft-core potential in the classical two-electron model to study the SDI of Ar by the elliptical laser pulses.

The Hamiltonian of the two-electron atom in the Heisenberg-core potential classical model (HPCM) is (atomic units are used throughout this Letter until stated otherwise)

$$H_1 = \frac{1}{|\mathbf{r}_1 - \mathbf{r}_2|} + \sum_{i=1,2}\left[-\frac{2}{r_i} + \frac{\mathbf{p}_i^2}{2} + V_H(r_i, p_i)\right], \quad (1)$$

where $\mathbf{r}_i$ and $\mathbf{p}_i$ are the position and canonical momentum of the ith electron, respectively. $V_H(r_i, p_i)$ is the Heisenberg-core potential, which is expressed as [25]

$$V_H(r_i, p_i) = \frac{\xi^2}{4\alpha r_i^2}\exp\left\{\alpha\left[1 - \left(\frac{r_i p_i}{\xi}\right)^4\right]\right\}. \quad (2)$$

The parameter α indicates the rigidity of the Heisenberg core, and the results of our calculations do not depend on this parameter. For a given α, the parameter ξ is chosen to match the second ionization potential of the target; i.e., it is set to make the minimum of the one-electron Hamiltonian $[H_2 = \frac{-2}{\mathbf{r}_1} + \frac{\mathbf{p}_1^2}{2} + V_H(r_1, p_1)]$ equal to the second ionization potential of Ar (-1.01 a.u.). For $\alpha = 2$, we obtain $\xi = 1.225$. For the two-electron atom, in Refs. [25–27], the ground-state energy of the system is obtained by minimizing the Hamiltonian H_1. In that configuration, the two electrons are located at opposite sides of the nucleus, and they are stationary to each other [25]. Differently, in our calculation, we employed the approach used by Eberly *et al.* [16] to determine the ground-state energy of the atom, i.e., by inputting an energy that equals to the sum of the first and the second ionization potentials of the target (-1.59 a.u. for Ar). The initial distributions of the ground-state atom in the phase space are obtained with the approach in the SPCM [17,18]. Figures 1(a) and 1(b) display the position distributions of the ground-state atom. We state that, in our calculation, the second ionization potential is related to the minimum of H_2 while the ground-state energy of the atom is determined by the "input" energy, which is higher than the minimal value of H_1. Thus, the two electrons are not fixed at two certain

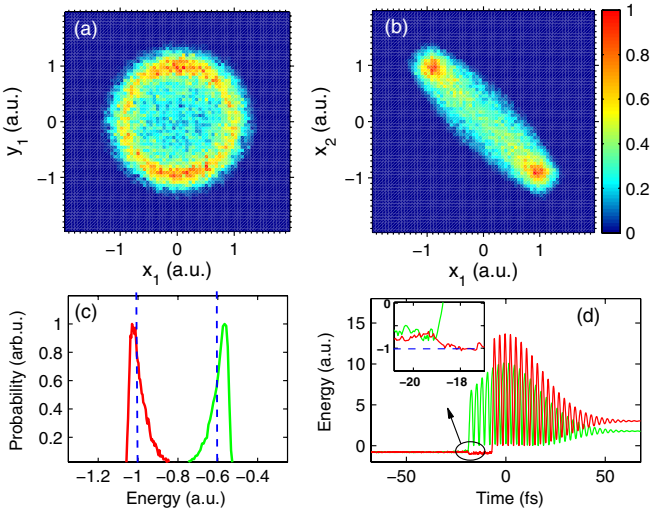

FIG. 1 (color online). (a),(b) The initial position distributions of electrons in the HPCM, where the initial energy of the system is set to be -1.59 a.u. The parameters of the Heisenberg core are $\alpha = 2$ and $\xi = 1.225$. Here, (x_i, y_i, z_i) represent the coordinates of the ith electron in the directions of the $\hat{x}$, $\hat{y}$, and $\hat{z}$ axes, respectively. (c) The ionization energy distributions of the first [the right-hand (green) curve] and the second [the left-hand (red) curve] electrons. The dashed blue lines (located at -0.6 and -1.0 a.u., respectively) are added to guide the eyes. (d) The energy evolution of the electrons for an illustrative SDI trajectory.

points but distributed in a finite region of the phase space [see Figs. 1(a) and 1(b)]. This relaxation of the position of the electron pairs in the phase space allows sufficient electron correlations in the initial state and during the ionization of the first electron.

The Hamiltonian of the two-electron atom in the presence of the laser field is

$$H = H_1 + (\mathbf{r}_1 + \mathbf{r}_2) \bullet \mathbf{E}(t), \quad (3)$$

where $\mathbf{E}(t)$ is the electric field of the laser pulses. The evolution of the system in the laser field is determined by the following equations:

$$\frac{d\mathbf{r}_i}{dt} = \frac{\partial H}{\partial \mathbf{p}_i}, \qquad \frac{d\mathbf{p}_i}{dt} = -\frac{\partial H}{\partial \mathbf{r}_i}. \quad (4)$$

The electric field is given as $\mathbf{E}(t) = f(t)[\frac{\varepsilon}{\sqrt{\varepsilon^2+1}} \times \cos(\omega t + \varphi)\hat{\mathbf{x}} + \frac{1}{\sqrt{\varepsilon^2+1}}\sin(\omega t + \varphi)\hat{\mathbf{y}}]$, where $f(t) = E_0 \exp[-\frac{1}{2}(\frac{t}{\tau})^2]$ is the field envelope. ω, ε, and φ are the laser frequency, the ellipticity, and the carrier-envelope phase, respectively. $2\sqrt{\ln 2}\tau$ denotes the pulse duration (FWHM).

First of all, we perform a calculation to test how well the first and second ionization potentials of Ar have been produced by this HPCM. The two-electron atoms are exposed to a 33-fs, 788-nm laser pulse with the intensity $I = 4.0$ PW/cm^2 and ellipticity $\epsilon = 0.77$. We trace the energy evolutions of the two electrons and record the energy of the second electron when the first electron is

ionized. This energy is assumed to be the second ionization potential of the model atom, which is shown in Fig. 1(c). The energy distribution of the first electron is also shown in Fig. 1(c), obtained by subtracting the energy of the second from the initial energy of the two-electron atom (-1.59 a.u.). It is clearly shown that the energy distributions of the first and second electrons peak at about -0.57 and -1.02 a.u. (almost at the bottom of Hamiltonian H_2), respectively, very close to the realistic first and second ionization potentials of Ar.

A recent experiment has shown that in SDI of Ar by strong elliptical laser pulses the ratio of the parallel and antiparallel electron emissions along the minor elliptical axis exhibits an oscillating behavior as a function of laser intensity [21]. This behavior has been predicted by the SPCM and explained as a multielectron effect beyond independent-electron assumption [20]. We display our calculations with the HPCM in Fig. 2, where the oscillating behavior is also clear. It implies that the electron correlations in SDI are included and represented in this HPCM. One can clearly see from Fig. 2 that at the high laser intensities the oscillating curve is a bit below 1, meaning the two electrons prefer to emit into the opposite hemispheres. This behavior agrees well with the experimental data {see Fig. 2(a) of Ref. [21]}.

In Figs. 3(a) and 3(d), we display the ion momentum distributions in the polarization plane for SDI of Ar by 33-fs laser pulses with laser intensities of 1.0 PW/cm^2 and 4.0 PW/cm^2, respectively. The ellipticity and wavelength are respectively 0.77 and 788 nm, the same as those in the recent experiment [11]. In the direction of the minor elliptical axis ($\hat{x}$ axis), the distribution exhibits a three-band structure at the relatively low laser intensity and a four-band structure at the relatively high laser intensity. Like that in the experiment, there is also a bifurcation from a three-band to a four-band structure in the intensity-dependent ion momentum distribution (not shown here). In the direction of the major elliptical axis ($\hat{y}$ axis), as shown in Figs. 3(c) and 3(f), the spectra show a Gaussian shape for both intensities. These results agree well with the experiment [11]. The origin of the four-band structure is interpreted as due to the different values of the electric field at which the two electrons are released [28,29]. Because of the ellipticity, the electrons preferentially ionize along the major axis, leading to the electrons with final momenta along the minor axis. The two outer bands in Fig. 3(d) correspond to the events where the two electrons emit into the parallel directions, whereas the two inner bands result from the events where the two electrons release into the antiparallel directions. At the relatively low laser intensity, the momentum amplitudes of the two electrons are almost the same because both electrons are ionized around the pulse center [11]. Thus, the antiparallel electron emissions result in the nearly zero momentum of the ion, leading to the three-band structure in ion momentum distribution [Fig. 3(a)]. The above picture for the intensity-dependent ion momentum spectra has been confirmed by back analyzing the SDI trajectories of our calculations (not shown here).

Figure. 4(a) displays the correlated radial momentum distribution of the electron pairs from SDI of Ar. The laser parameters are the same as those in Fig. 3(d). Note that in this calculation the focal volume effect assuming a Gaussian beam profile has been considered. The momentum p'_r in Fig. 4(a) is defined as $p'_r = \sqrt{[(\epsilon^2+1)/\epsilon^2]p_x^2 + (\epsilon^2+1)p_y^2}$, which is an

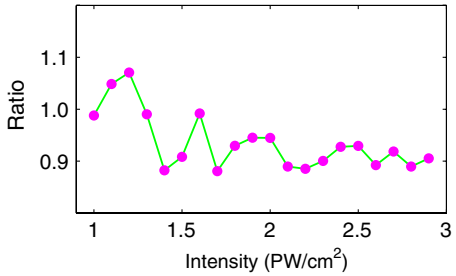

FIG. 2 (color online). The ratio of SDI electron counts of parallel and antiparallel emissions along the minor elliptical axis ($\hat{x}$ axis) of the laser pulses, as a function of laser intensity. The laser parameters are the same as those in Ref. [21]; i.e., the duration, wavelength, and ellipticity of the pulses are 7 fs, 740 nm, and 0.78, respectively. The results are obtained by averaging over the carrier-envelope phase between 0 and 2π.

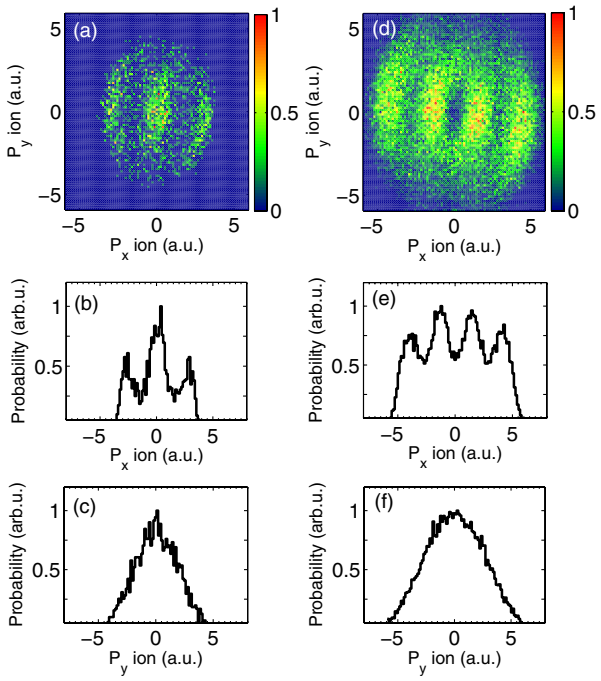

FIG. 3 (color online). The ion momentum distributions in the polarization plane for the SDI of Ar at laser intensities of (a) 1.0 PW/cm^2 and (d) 4.0 PW/cm^2. (b) and (c) show the ion momentum spectra along the minor and major axes of the polarization, obtained by integrating the distributions in (a) over p_y and p_x, respectively. (e) and (f) are the same as (b) and (c) but for the distribution in (d). The pulse durations are 33 fs.

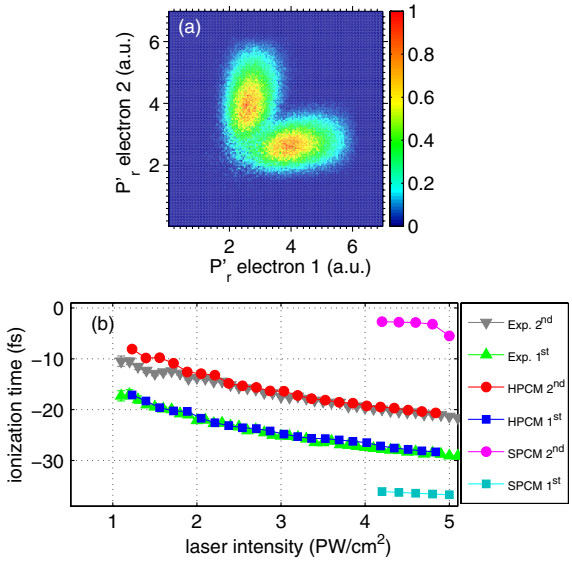

FIG. 4 (color online). (a) The electron correlation spectrum for the momentum p'_r. The laser intensity is 4.0 PW/cm^2. (b) The release times of the first [upper (blue) squares] and the second [lower (red) circles] electrons in SDI (for the 33-fs pulses), which are extracted from the electron momentum p'_r (see the text for details). The experimental data from Ref. [11] (triangles) are also shown in (b). For comparison, we also displayed the numerical results from the SPCM [the upper (magenta) circles and the lower (cyan) squares]. In our calculations, the collected DI events range from 10^4 to 10^5, depending on the peak intensity, and then the statistical error is negligible.

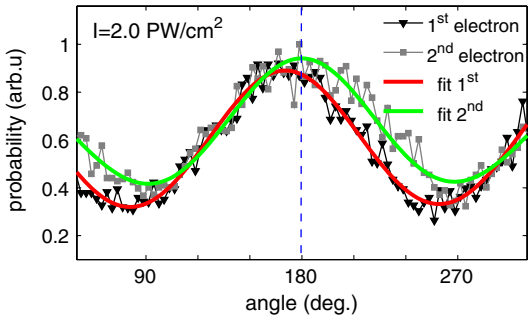

FIG. 5 (color online). The angular distributions of the two electrons from SDI by the 33-fs elliptical ($\varepsilon = 0.77$) laser pulses. The solid lines correspond to the Gaussian fitting of the distributions. The dashed line is added to guide the eyes.

injective function of time under the condition that the electron must ionize before the peak of the pulse [11]. The repulsion behavior along the diagonal means that the two electrons achieve different final momenta at the end of the pulses, implying the different release times of the two electrons. In Ref. [11], the ionization times of the two electrons in SDI are read from the electron's final momentum p'_r. It is found that the ionization time for the first electron agrees well with the prediction of the independent-electron model. However, the ionization of the second electron occurs much earlier than the prediction of the independent-electron model. With the same procedure as that in Ref. [11], we extract the release times of two electrons in our classical simulations. The results are shown in Fig. 4(b), where the experimental data from Ref. [11] are also displayed. Note that for our numerical results, the laser intensities in Fig. 4(b) are scaled with a constant factor of 0.82, which is well in the experimental uncertainty range. Surprisingly, the release times from our classical simulations agree very well with the experimental data, both for the first and the second electrons. For comparison, we have repeated the calculations above with the SPCM. The ionization times of the first and the second electrons from the SPCM [as shown in Fig. 4(b)] seriously deviate from the experimental data. Here, we only displayed the results at intensities above 4.0 PW/cm^2 because in the SPCM the DI yield is very low at relatively low intensities (the DI probability does not exceed 1% until the laser intensity reaches 4.0 PW/cm^2). Note that such quantitative agreement between the experimental results and our numerical results also works well for the short 7-fs pulses. During the past decades, classical methods have been widely employed to describe the strong-field phenomena. However, they stand at the qualitative point of view. As far as we know, our calculation is the first successful example of the quantitative investigation of the strong-field DI with a classical treatment.

For the theoretical treatment of the independent-electron model in Ref. [11], the Coulomb interaction between the ion and the escaping electron is neglected. Here, we estimate how strongly the Coulomb interaction affects the release-time reading. It has been demonstrated that the angular distributions of the electrons can serve as a signal to estimate the importance of the Coulomb interaction on the electrons [30,31]. In Fig. 5, we display the angular spectra of the first and the second electrons. Note that the angular spectra peak at 180° (and 0°) if there is no interaction between the ion and the escaping electron. Figure 5 shows that the spectrum of the first electron [the lower (red) curve] peaks at an angle slightly deviating from 180°, indicating a weak Coulomb correction on the electron trajectory [30,31]. For the second electron [the upper (green) curve], however, the spectrum peaks almost at 180°, implying negligible Coulomb interaction between the ion and escaping electron. These results indicate that the influence of the Coulomb attraction on the second electron is even weaker than that on the first electron. Thus, it confirms that the Coulomb attraction has negligible contribution to the deviation between the experimental measurement and independent-electron prediction for the ionization time of the second electron reported in Ref. [11].

It has been proposed that inelastic tunneling [32,33], where the first electron escapes, leaving the core in an excited state, is important in double and multiple ionization at high laser intensities. However, the most general picture of the ionization process revealed by our classical model is that the first electron ionizes, leaving the second electron at the ground state of Ar^+, as shown in Fig. 1(d) [see the inset

of Fig. 1(d)]. Note that the second electron stays at a state with an energy higher than -1.01 a.u. after the first ionization for a small part of the SDI trajectories shown in Fig. 1(c). This "excitation" is responsible for the oscillation behavior of the parallel-antiparallel ratio (see Fig. 2) [20]. However, it is not responsible for the early release time of the second electron because the second ionization time shown in Fig. 4(b) does not change when these trajectories are excluded. It is also speculated that the deviation of the independent-electron prediction of the second ionization from the measured data [11] is possibly attributed to the empirical formula for the ionization rate [34], which may be inaccurate in the experimental condition where the nonadiabatical effect is important to the ionization process [35]. Then, it is not clear to what extent the deviation of the second ionization time comes from the inaccuracy of the ionization rate formula and to what extent the electron correlations influence the ionization of the second electron. These questions call for more detailed investigations.

In conclusion, we have investigated SDI of Ar by the elliptical laser pulses with the HPCM in which the electron correlation is included during the entire process. The experimental observed ion momentum spectra and oscillating behavior of the ratio of the antiparallel to parallel electron emissions are well reproduced by this classical model. Especially, the measured ionization time of the second electron, which strongly deviates from the prediction of the standard independent-electron model, is excellently reproduced by the HPCM. The quantitative agreement between our classical calculations and experimental results provides strong support to the classical treatment of the multielectron processes induced by strong laser fields, which is currently indispensable because the nonperturbative quantum treatments of the complex effect are not feasible.

We acknowledge helpful discussions with Dr. A. N. Pfeiffer, Dr. X. Wang, and Professor J. H. Eberly. We thank Dr. Pfeiffer for providing experimental data. This work was supported by the National Science Fund (No. 60925021 and No. 11004070) and the 973 Program of China (No. 2011CB808103).

Note added in proof.—Recently, Wang *et al.* [36] also reproduced the release times in SDI with the SPCM by artificially adjusting the ionization potentials of the model atom to those of the investigated target.

*Corresponding author
lupeixiang@mail.hust.edu.cn

[1] P. B. Corkum, Phys. Rev. Lett. **71**, 1994 (1993).
[2] K. C. Kulander, J. Cooper, and K. J. Schafer, Phys. Rev. A **51**, 561 (1995).
[3] Th. Weber, H. Giessen, M. Weckenbrock, G. Urbasch, A. Staudte, L. Spielberger, O. Jagutzki, V. Mergel, M. Vollmer, and R. Dörner, Nature (London) **405**, 658 (2000).
[4] A. Rudenko, K. Zrost, B. Feuerstein, V. L. B. de Jesus, C. D. Schröter, R. Moshammer, and J. Ullrich, Phys. Rev. Lett. **93**, 253001 (2004).
[5] A. Becker, R. Dörner, and R. Moshammer, J. Phys. B **38**, S753 (2005).
[6] Y. Zhou, C. Huang, A. Tong, Q. Liao, and P. Lu, Opt. Express **19**, 2301 (2011).
[7] R. Kopold, W. Becker, H. Rottke, and W. Sandner, Phys. Rev. Lett. **85**, 3781 (2000).
[8] C. Ruiz, L. Plaja, L. Roso, and A. Becker, Phys. Rev. Lett. **96**, 053001 (2006).
[9] J. S. Prauzner-Bechcicki, K. Sacha, B. Eckhardt, and J. Zakrzewski, Phys. Rev. Lett. **98**, 203002 (2007).
[10] A. Fleischer, H. J. Wörner, L. Arissian, L. R. Liu, M. Meckel, A. Rippert, R. Dörner, D. M. Villeneuve, P. B. Corkum, and A. Staudte, Phys. Rev. Lett. **107**, 113003 (2011).
[11] A. N. Pfeiffer, C. Cirelli, M. Smolarski, R. Dörner, and U. Keller, Nature Phys. **7**, 428 (2011).
[12] J. S. Parker, B. J. S. Doherty, K. T. Taylor, K. D. Schultz, C. I. Blaga, and L. F. DiMauro, Phys. Rev. Lett. **96**, 133001 (2006).
[13] R. V. Jensen, Phys. Rev. A **30**, 386 (1984).
[14] J. G. Leopoldt and D. Richards, J. Phys. B **24**, 1209 (1991).
[15] K. Sacha and B. Eckhardt, Phys. Rev. A **63**, 043414 (2001).
[16] P. J. Ho, R. Panfili, S. L. Haan, and J. H. Eberly, Phys. Rev. Lett. **94**, 093002 (2005).
[17] S. L. Haan, L. Breen, A. Karim, and J. H. Eberly, Phys. Rev. Lett. **97**, 103008 (2006).
[18] Y. Zhou, Q. Liao, and P. Lu, Phys. Rev. A **80**, 023412 (2009).
[19] Y. Zhou, Q. Liao, and P. Lu, Phys. Rev. A **82**, 053402 (2010).
[20] X. Wang and J. H. Eberly, arXiv:1102.0221v1.
[21] A. N. Pfeiffer, C. Cirelli, M. Smolarski, X. Wang, J. H. Eberly, R. Dörner, and U. Keller, New J. Phys. **13**, 093008 (2011).
[22] K. Ueda and K. L. Ishikawa, Nature Phys. **7**, 371 (2011).
[23] D. Bauer, Phys. Rev. A **56**, 3028 (1997).
[24] Y. Zhou, Q. Liao, P. Lan, and P. Lu, Chin. Phys. Lett. **25**, 3950 (2008).
[25] C. L. Kirschbaum and L. Wilets, Phys. Rev. A **21**, 834 (1980).
[26] D. Zajfman and D. Maor, Phys. Rev. Lett. **56**, 320 (1986).
[27] P. B. Lerner, K. J. LaGattuta, and J. S. Cohen, Phys. Rev. A **49**, R12 (1994).
[28] C. M. Maharjan, A. S. Alnaser, X. M. Tong, B. Ulrich, P. Ranitovic, S. Ghimire, Z. Chang, I. V. Litvinyuk, and C. L. Cocke, Phys. Rev. A **72**, 041403(R) (2005).
[29] X. Wang and J. H. Eberly, Phys. Rev. Lett. **103**, 103007 (2009).
[30] S. V. Popruzhenko, G. G. Paulus, and D. Bauer, Phys. Rev. A **77**, 053409 (2008).
[31] A. N. Pfeiffer, C. Cirelli, M. Smolarski, D. Dimitrovski, M. Abu-samha, L. B. Madsen, and U. Keller, Nature Phys. **8**, 76 (2011).
[32] A. S. Kornev, E. B. Tulenko, and B. A. Zon, Phys. Rev. A **68**, 043414 (2003).
[33] W. A. Bryan *et al.*, Nature Phys. **2**, 379 (2006).
[34] X. M. Tong and C. D. Lin, J. Phys. B **38**, 2593 (2005).
[35] I. Barth and O. Smirnova, Phys. Rev. A **84**, 063415 (2011).
[36] X. Wang, J. Tian, and J. H. Eberly (private communication).